

ORIGINAL RESEARCH PAPER

Investigation of Heat Transfer Enhancement or Deterioration of Variable Properties Al₂O₃-EG-water Nanofluid in Buoyancy Driven Convection

H. Khorasanizadeh¹, M. M. Fakhari¹, S. P. Ghaffari^{1,*}

¹ Department of Thermo-fluids, Faculty of Mechanical Engineering, University of Kashan, Kashan, I.R. Iran

ARTICLE INFO:

Article history:

Received 4 April 2013

Accepted 24 November 2013

Keywords:

Enclosure

Ethylene Glycol

Nanofluid

Natural Convection

Nusselt Number

Variable Properties,

Abstract

In this study, the natural convection heat transfer of variable properties Al₂O₃-EG-water nanofluid in a differentially heated rectangular cavity has been investigated numerically. The governing equations, for a Newtonian fluid, have been solved numerically with a finite volume approach. The influences of the pertinent parameters such as Ra in the range of 10^3 - 10^7 and volume fraction of nanoparticles from 0 to 0.04 on heat transfer characteristics have been studied. The results verified by making overall comparison with some existing experimental results have shown that for $Ra=10^3$, for which conduction heat transfer is dominant, the average Nusselt number increases as volume fraction of nanoparticles increases, but for higher Ra numbers in contradiction with the constant properties cases it decreases. This reduction, which is associated with increased viscosity, is more severe at Ra of 10^4 compared to higher Ra numbers such that the least deterioration in heat transfer occurs for $Ra=10^7$. This is due to the fact that as Ra increases, the Brownian motion enhances; thus conductivity improves and becomes more important than viscosity increase. An scale analysis, performed to clarify the contradictory reports in the literature on the natural convection heat transfer enhancement or deterioration of nanofluids, showed that different kinds of evaluating the base fluid Rayleigh number has led to such a difference.

1. Introduction

An innovative technique to enhance heat transfer is using nano-scale particles in the base fluid. During the two last decades nanofluids, which are engineered colloids composed of nanometer-sized particles

suspended in traditional heat transfer fluids, have been studied extensively. Remarkable increase for thermal conductivity of nanofluids can be achieved even at low volume fraction of nanoparticles. This is why nanofluids have attracted the attention of the heat transfer community. Experimental and numerical results show that, in forced convection and for a given Reynolds number, the convective heat transfer coefficient increases by increasing the nanoparticles

*Corresponding author

Email Address: Payam_ghaffary@yahoo.com

volume fraction [1-4]. However, enhancement of natural convection heat transfer by using a nanofluid is still controversial. Examples of the controversial results are those reported by Khanafer et al. [5]. They were among the first investigators to conduct a

numerical study of the heat transfer enhancement in a two-dimensional enclosure utilizing nanofluids for various pertinent parameters. They tested different models for nanofluid density, viscosity and thermal

Nomenclature		Greek Symbols	
c_p	specific heat at constant pressure ($J\ kg^{-1}\ K^{-1}$)	α	thermal diffusivity ($m^2\ s^{-1}$)
d	diameter (m)	β	thermal expansion coefficient (K^{-1})
g	gravitational acceleration ($m\ s^{-2}$)	θ	dimensionless temperature
h	heat transfer coefficient ($W\ m^{-2}\ K^{-1}$)	κ	Boltzmann constant, $1.3806503 \times 10^{-23}$, ($J\ K^{-1}$)
H	height of the cavity (m)	μ	viscosity (Pa s)
k	thermal conductivity ($W\ m^{-1}\ K^{-1}$)	ξ	Ethylene Glycol volumetric concentration
L	length of the cavity (m)	ρ	density ($kg\ m^{-3}$)
Nu	local Nusselt number	Φ	volume fraction of nanoparticles
Nu_{avg}	average Nusselt number	ψ	stream function
Nu_{avg}^*	average Nusselt number ratio	Subscripts	
P	pressure (Pa)	avg	average
Pr	Prandtl number	C	cold
Ra	Rayleigh number	EG	Ethylene Glycol
T	temperature (K)	f	Base fluid
u, v	dimensional x and y components of velocity ($m\ s^{-1}$)	H	Hot
x, y	dimensional coordinates (m)	m	mean
X, Y	dimensionless coordinates	nf	Nanofluid
t	Time (s)	o	properties at reference temperature
		P	nanoparticle
		w	water
		superscripts	
		*	dimensionless properties

expansion coefficients. It was found that the suspended nanoparticles substantially increase the heat transfer rate at any given Grashof number. Recently, Lin and Violi [6], Sheikzadeh et al. [7] as well as Jahanshahi et al. [8] showed similar trend. Santra et al. [9] studied heat transfer characteristics of Cu-water nanofluid in a differentially heated square cavity by treating the nanofluid as a non-Newtonian fluid and reported decrease in heat transfer by increasing the volume fraction of nanoparticles at a particular Rayleigh number. Ho et al. [10] reported a numerical simulation of natural convection of a nanofluid in a square enclosure considering the effects due to uncertainties of viscosity and thermal conductivity by considering two models for viscosity

and thermal conductivity. They reported that a significant difference between predictions of viscosity models leads to contradictory heat transfer efficacy of nanofluid; so that the heat transfer across the enclosure can be found to be enhanced or deteriorated with respect to the base fluid. Moreover Abu-Nada et al. [11] demonstrated that the enhancement of heat transfer in natural convection depends mainly on Rayleigh number. For a certain Rayleigh number, like $Ra=104$, the heat transfer was not sensitive to increased volume fraction of nanoparticles, whereas at higher Rayleigh numbers an enhancement in heat transfer was observed. On the other hand, the experimental findings reported by Putra et al. [12] and Li and Peterson [13] demonstrated deterioration in

heat transfer by increasing the volume fraction of nanoparticles. Ho et al. [14] through their experiments observed a deterioration in heat transfer for >0.02 , but almost 18% enhancement for $=0.001$, however, they did not give an explanation for such an enhancement. Similar observations were reported experimentally by Nnanna [15]. His results showed that for small volume fractions (0.002–0.02) the presence of the nanoparticles does not impede the free convective heat transfer, rather it augments the rate of heat transfer, but for volume fractions higher than 0.02, the convective heat transfer coefficient declines due to reduction in the Rayleigh number caused by increased kinematic viscosity. Khanafer and Vafai [16] used the experimental results of Ho et al. [14] to explain the heat transfer behavior of Al_2O_3 -water nanofluid. According to their findings, higher volume fractions of nanoparticles cause an increase in the viscous force of the nanofluid and consequently heat transfer is suppressed. Also, as the nanoparticles diameter increases the ratio of the Rayleigh number of nanofluid to that of the base fluid decreases. Although Khanafer and Vafai [16] were successful to explain some heat transfer behaviors of Al_2O_3 -water nanofluid, they mentioned: “Additional theoretical and experimental research studies are required to clarify the mechanisms responsible for heat transfer enhancement in nanofluids.”

As for nanofluid thermophysical properties, the aforementioned numerical works relied on the models not sensitive to the temperature. Recently, Abu-Nada and Chamkha [17] studied the natural convection heat transfer characteristics in a differentially heated enclosure filled with CuO -EG-water nanofluid by using different variable thermal conductivity and viscosity models. Their results showed deterioration of the average Nusselt number as the volume fraction of nanoparticles increased depending on the combination of CuO -EG-water thermal conductivity and viscosity models employed for $\text{Ra}=104$ and 105 . Moreover, in another study Abu-Nada et al. [18] investigated the role of variable properties of Al_2O_3 -water and CuO -water nanofluids in differentially heated enclosures and found that variation of properties play a major role on the heat transfer rate. They considered Ra in the range of 103 - 105 and for Al_2O_3 -water at high Rayleigh numbers reported that Nusselt number deteriorated by increasing the volume fraction of nanoparticles above 0.05 , but at low nanoparticles volume fractions a fluctuation in heat transfer was registered. However, for CuO -water at

high Rayleigh numbers a continuous decrease in Nusselt number was noticed as the volume fraction of nanoparticles increased, but it was not sensitive to the volume fraction at low Rayleigh numbers. Recently, Sahoo et al. [19] studied the effect of nanoparticles volume fraction on nanofluids viscosity under a wide range of temperatures, experimentally. The nanofluid used in their experiments was a mixture of 60:40 (by mass) Ethylene Glycol and water containing Al_2O_3 nanoparticles. They inferred that the viscosity drops with temperature for different volume fractions of nanoparticles. Also Vajjha and Das [20, 21] and Vajjha et al. [22] experimentally investigated the thermal conductivity and specific heat of nanofluids comprised of Al_2O_3 nanoparticles suspended in a 60:40 (by mass) EG-water mixture under a wide range of temperatures. Therefore, from physical point of view the dependence of nanofluid properties on temperature and volume fraction of nanoparticles is very important and the previous investigations designate that it must be taken into account.

...The present numerical study tries to shed light on the reason for existing controversies about the results presented in the literature on the natural heat transfer behavior of nanofluids. In particular, in [17-18] different behaviors have been reported for volume fractions less than 0.05 and the explanation presented in [18] do not seem satisfactory; hence this matter is clarified at this juncture correspondingly. For this purpose Al_2O_3 -EG-water nanofluid is used and as for its thermophysical properties recent experimental correlations reported in [19-22] for nanoparticles diameter of 44 nm are used. Also unlike [18], the heat transfer characteristics are evaluated for a wider range of Rayleigh numbers from 103 up to 107 with volume fractions of nanoparticles from 0.0 to 0.04 . Furthermore, for justification of the new findings a scale analysis is performed also the results are compared with the cases in which constant properties for nanofluid have been employed.

2. Problem statement and boundary conditions

A schematic view of the cavity considered in the present study is shown in Fig. 1. The length and the height of the cavity are denoted by L and H ($L = H$), respectively. The left vertical wall of the cavity is kept at a temperature (T_H) higher than the right constant cold wall temperature (T_C).

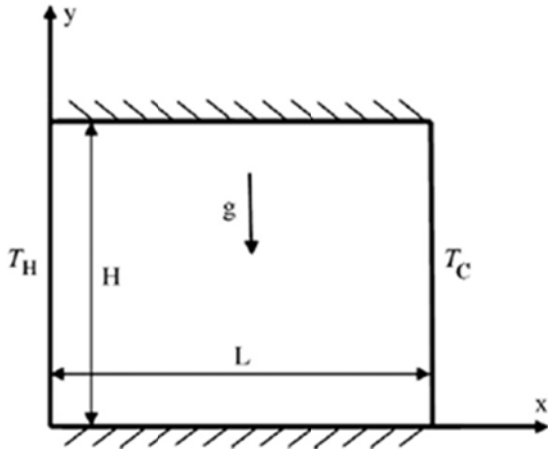


Fig. 1. A schematic diagram of the physical model.

The boundary conditions are:

$$u = v = \frac{\partial T}{\partial y} = 0 \text{ at } 0 \leq x \leq L \text{ and } y = 0, H \quad (1-a)$$

$$u = v = 0, T = T_H \text{ at } x = 0 \text{ and } 0 \leq y \leq H \quad (1-b)$$

$$u = v = 0, T = T_C \text{ at } x = L \text{ and } 0 \leq y \leq H \quad (1-c)$$

The fluid in the enclosure is a mixture of 60:40 (by mass) Ethylene Glycol and water containing Al_2O_3 nanoparticles. The nanofluid is assumed incompressible and the flow is considered two-dimensional and laminar. The density variation in the buoyancy term is approximated by the Boussinesq model. According to [19] the nanofluid exhibits a non-Newtonian behavior at a low temperature range of 238 to 273 K for all volume fractions of nanoparticles, such that it behaves as a Bingham plastic with small yield stress that decreases with decreasing volume fraction of nanoparticles and increases with increasing temperature. However, the nanofluid in the temperature range of 273 to 363 K behaves as a Newtonian fluid. In this study, the simulations are in the temperature range of 298 to 313 K; so the nanofluid is considered Newtonian.

3. Mathematical formulation

The EG-water mixture and nanoparticles are assumed in thermal equilibrium and no slip occurs between the two media. So, the governing equations for the laminar and steady state natural convection using variable properties are given as:

Continuity:

$$\frac{\partial(\rho_{nf}u)}{\partial x} + \frac{\partial(\rho_{nf}v)}{\partial y} = 0 \quad (2)$$

x-momentum equation:

$$\frac{\partial}{\partial x}(\rho_{nf}uu) + \frac{\partial}{\partial y}(\rho_{nf}vu) = -\frac{\partial p}{\partial x} + \frac{\partial}{\partial x}\left(\mu_{nf}\frac{\partial u}{\partial x}\right) + \frac{\partial}{\partial y}\left(\mu_{nf}\frac{\partial u}{\partial y}\right) \quad (3)$$

y-momentum equation:

$$\frac{\partial}{\partial x}(\rho_{nf}uv) + \frac{\partial}{\partial y}(\rho_{nf}vv) = -\frac{\partial p}{\partial y} + \frac{\partial}{\partial x}\left(\mu_{nf}\frac{\partial v}{\partial x}\right) + \frac{\partial}{\partial y}\left(\mu_{nf}\frac{\partial v}{\partial y}\right) + g(T - T_C)(\rho_{nf}\beta_{nf}) \quad (4)$$

Energy equation:

$$\frac{\partial}{\partial x}(\rho_{nf}uT) + \frac{\partial}{\partial y}(\rho_{nf}vT) = \frac{\partial}{\partial x}\left(\frac{k}{c_p}\frac{\partial T}{\partial x}\right) + \frac{\partial}{\partial y}\left(\frac{k}{c_p}\frac{\partial T}{\partial y}\right) \quad (5)$$

To rewrite the dimensional form of the equations in the non-dimensional form, the following dimensionless variables are used:

$$X = x/L, \quad Y = y/H, \quad U = uL/\alpha_{f,o}, \quad V = vL/\alpha_{f,o} \quad (6)$$

$$P = \frac{pL^2}{\rho_{f,o}\alpha_{f,o}^2}, \quad \theta = \frac{T - T_C}{T_H - T_C}, \quad \rho^* = \frac{\rho_{nf}}{\rho_{f,o}}, \quad \mu^* = \frac{\mu_{nf}}{\mu_{f,o}}$$

$$k^* = \frac{k_{nf}}{k_{f,o}}, \quad c_p^* = \frac{c_{pnf}}{c_{pf,o}}$$

Using the above dimensionless variables the non-dimensional form of the governing equations are:

$$\frac{\partial(\rho^*U)}{\partial X} + \frac{\partial(\rho^*V)}{\partial Y} = 0 \quad (7)$$

$$\frac{\partial}{\partial X}(\rho^*UU) + \frac{\partial}{\partial Y}(\rho^*VU) = -\frac{\partial P}{\partial X} + Pr_o \frac{\partial}{\partial X} \left(\mu^* \frac{\partial U}{\partial X} \right) + Pr_o \frac{\partial}{\partial Y} \left(\mu^* \frac{\partial U}{\partial Y} \right) \quad (8)$$

$$\frac{\partial}{\partial X}(\rho^*UV) + \frac{\partial}{\partial Y}(\rho^*VV) = -\frac{\partial P}{\partial Y} + Pr_o \frac{\partial}{\partial X} \left(\mu^* \frac{\partial v}{\partial x} \right) + pr_o \frac{\partial}{\partial y} \left(\mu^* \frac{\partial v}{\partial y} \right) + Ra \cdot pr_o \theta (\rho^* \beta^*) \tag{9}$$

$$\frac{\partial}{\partial X}(\rho^*U\theta) + \frac{\partial}{\partial Y}(\rho^*V\theta) = \frac{\partial}{\partial X} \left(\frac{k^*}{c_p^*} \frac{\partial \theta}{\partial X} \right) + \frac{\partial}{\partial y} \left(\frac{k^*}{c_p^*} \frac{\partial \theta}{\partial y} \right) \tag{10}$$

where the Rayleigh and Prandtl are:

$$Pr_o = \frac{\mu_{f,o} c_{p_{f,o}}}{k_{f,o}}, \quad Ra = \frac{g \beta_{f,o} L^3 (T_H - T_C)}{\alpha_{f,o} \nu_{f,o}} \tag{11}$$

The boundary conditions in the dimensionless form are:

$$U = V = \frac{\partial \theta}{\partial Y} = 0 \text{ at } 0 \leq X \leq 1 \text{ and } Y = 0, 1 \tag{12-a}$$

$$U = V = 0, \theta = 1 \text{ at } X = 0 \text{ and } 0 \leq Y \leq 1 \tag{12-b}$$

$$U = V = 0, \theta = 0 \text{ at } X = 1 \text{ and } 0 \leq Y \leq 1 \tag{12-c}$$

The convective heat transfer coefficient on any y at the hot wall is:

$$h = -k_{nf} \left. \frac{\partial T}{\partial x} \right|_{x=0} \tag{13}$$

and the local Nusselt number is:

$$Nu = \frac{hL}{k_f} \tag{14}$$

Substituting Eq. (13) into Eq. (14) and using the dimensionless quantities, the local Nusselt number along the left wall becomes:

$$Nu = - \left(\frac{k_{nf}}{k_{f,o}} \right) \left. \frac{\partial \theta}{\partial X} \right|_{X=0} \tag{15}$$

where k_{nf} in constant properties and in variable properties models are evaluated using Eq. (22) and Eq. (25), respectively. The average Nusselt number on the hot wall is:

$$Nu_{avg} = \int_0^1 Nu \, dY \tag{16}$$

And the average Nusselt number ratio is defined as:

$$Nu_{avg}^* = \frac{Nu_{avg,nf}}{Nu_{avg,f}} \tag{17}$$

4. Thermophysical properties of nanofluids

The aim of this work is examination of heat transfer characteristics of the Al₂O₃-EG-water nanofluid using temperature dependent models for the properties. However, to show the importance of properties variations the results are compared with those of constant properties models. In this section both variable and constant properties models used in this study are introduced.

4.1. Constant properties models

The effective density of nanofluids, validated experimentally for Al₂O₃-water nanofluid by Pak and Cho [23], is given by:

$$\rho_{nf} = \Phi \rho_p + (1 - \Phi) \rho_f \tag{18}$$

The specific heat and thermal expansion coefficient of nanofluids proposed by [5, 24], respectively, are:

$$(\rho c_p)_{nf} = (1 - \Phi)(\rho c_p)_f + \Phi(\rho c_p)_p \tag{19}$$

$$(\rho \beta)_{nf} = (1 - \Phi)(\rho \beta)_f + \Phi(\rho \beta)_p \tag{20}$$

The nanofluid viscosity is estimated by the following correlation developed by Brinkman [25] as:

$$\mu_{nf} = \frac{\mu_f}{(1 - \Phi)^{2.5}} \tag{21}$$

For thermal conductivity of nanofluids numerous theoretical studies have been conducted dating back

to the classical work of Maxwell. Maxwell's model states that the effective thermal conductivity of a nanofluid depends on the thermal conductivity of both nanoparticles and the base fluid as well as the volume fraction of nanoparticles, irrespective of the nanoparticles mean diameter. Accordingly, the effective thermal conductivity, given by Wang et al. [26], is:

$$k_{nf,Maxwell} = \frac{k_p + 2k_f - 2\Phi(k_f - k_p)}{k_p + 2k_f + \Phi(k_f - k_p)} k_f \quad (22)$$

For the mixture of EG and water:

$$\rho_f = \xi\rho_{EG} + (1 - \xi)\rho_w \quad (23-a)$$

$$(\rho\eta)_f = \xi(\rho\eta)_{EG} + (1 - \xi)(\rho\eta)_w \quad (23-b)$$

Where η is the fluid thermophysical property and ξ is Ethylene Glycol volumetric concentration in the mixture, which is equal to 0.578 for 60:40 EG/w by mass mixture [27]. The properties of nanoparticles, Ethylene Glycol and water at reference temperature are presented in Table 1.

Table 1
Gas phase and Surface Reactions

Properties	Al ₂ O ₃	EG	Water
ρ (kg m ⁻³)	3970	1114.4	997
c_p (J kg ⁻¹ K ⁻¹)	765	2415	4179
$\mu \times 10^4$ (Pa s)	-	157	8.55
$\beta \times 10^5$ (K ⁻¹)	0.846	65	27.61
k (W m ⁻¹ K ⁻¹)	36	0.252	0.613

4.2. Variable properties models

As described by Vajjha et al. [22], the best correlation for the density of Al₂O₃ nanoparticles with nanoparticle mean diameter of 44 nm dispersed in 60:40 EG/w as the base fluid is presented by Eq. (18). In this correlation, the base fluid variable density proposed by [29] is used as:

$$\rho_f = -2.43 \times 10^{-3} T^2 + 0.96216T + 1009.9261 \quad (24)$$

The specific heat of Al₂O₃-EG-w nanofluid with nanoparticle mean diameter of 44 nm for 60:40 EG/w given by Vajjha and Das [21] is:

$$\frac{c_{p,nf}}{c_{p,f}} = \frac{8.911 \times 10^{-4} T + 0.5179 \frac{c_{p,p}}{c_{p,f}}}{0.425 + \Phi} \quad (25)$$

where the base fluid variable specific heat proposed by [29] is:

$$c_{p,f} = 4.2483T + 1882.4 \quad (26)$$

Sahoo et al. [19] measured the viscosity of Al₂O₃-EG-w nanofluid with nanoparticle mean diameter of 44 nm for volume fractions up to 0.1. For the temperature range of 273 to 363 K, they proposed:

$$\mu_{nf} = 2.392 \times 10^{-7} \exp\left(\frac{2903}{T} + 12.65\Phi\right) \quad (27)$$

Vajjha and Das [20] measured the thermal conductivity of Al₂O₃-EG-w nanofluid with nanoparticle mean diameter of 44 nm for 60:40 EG/w. They developed a thermal conductivity model as a two-term function in the temperature range of 298 to 363 K as:

$$k_{nf} = \frac{k_p + 2k_f - 2(k_f - k_p)\Phi}{k_p + 2k_f + 2(k_f - k_p)\Phi} k_f + 5 \times 10^4 \quad (28-a)$$

$$B\Phi\rho_f c_{p,f} \sqrt{\frac{KT}{\rho_p d_p}} f(T, \Phi)$$

where $f(T, \Phi)$ is:

$$f(T, \Phi) = \left(2.8217 \times 10^{-2} \Phi + 3.917 \times 10^{-3}\right) \frac{T}{T_0} + (-3.0669 + 10^{-2} \Phi - 3.91123 \times 10^{-23}) \quad (28-b)$$

B is fraction of the liquid volume which travels with a particle and for nanofluid comprised of Al₂O₃ nanoparticles is [20]:

$$B = 8.4407(100\Phi)^{-1.07304} \quad (28-c)$$

The first term in Eq. (28-a) is called the static part and the second term takes into account the effect of particle size, particle volume fraction, temperature and properties of the base fluid as well as the nanoparticles subjected to Brownian motion.

To the best of our knowledge, there is no correlation for thermal expansion coefficient of Al₂O₃-EG-w as a function of temperature; thus in this study Eq. (20) has been used as a base to obtain a variable thermal expansion coefficient. For this purpose, the values of density and thermal expansion coefficient of EG and water taken from [28], within the temperature range of 290-320 K, have been curve fitted firstly. The results are:

$$\rho_{EG} = 4.667 \times 10^{-4} T^3 - 0.4515 T^2 + 144.1 T - 1.408 \times 10^4 \quad (R^2 = 1) \quad (29)$$

$$\beta_{EG} = 6.5 \times 10^{-4} \quad (30)$$

$$\rho_w = -0.003404 T^2 + 1.726 T + 785.1 \quad (R^2 = 0.997) \quad (31)$$

$$\beta_w = (-0.06107 T^2 + 45.9 T - 7999) \times 10^{-6} \quad (R^2 = 1) \quad (32)$$

Then the thermal expansion coefficient of the EG/w mixture has been obtained using Eq. (23-b) and finally by substituting the results in Eq. (20) the thermal expansion coefficient of nanofluid has been obtained.

The other properties of the base fluid are [29]:

$$\mu_f = 5.55 \times 10^{-7} \exp\left(\frac{2664}{T}\right) \quad (33)$$

$$k_f = -3.196 \times 10^{-6} T^2 + 2.512 \times 10^{-3} T - 0.105 \quad (34)$$

5. Numerical procedure

The governing equations and the associated boundary conditions have been solved numerically using the finite volume method. The diffusion terms in the governing equations have been discretized using a second-order central difference scheme; while

a hybrid scheme (a combination of the central difference scheme and the upwind scheme) has been employed to approximate the convection terms. A staggered grid system together with the SIMPLER algorithm has been adopted to solve for the pressure and the velocity components. The coupled set of discretized equations has been solved iteratively using the TDMA method [30]. To obtain converged solution an under-relaxation scheme has been employed.

5.1. Benchmarking of the code

In order to validate the numerical procedure and as a test case, the geometry and conditions of Jahanshahi et al. [8] have been considered. The test case is the natural convection of SiO₂-water nanofluid in a two-dimensional square enclosure. Table 2 shows the average Nusselt number on the hot wall for $Ra=10^5$ obtained by the results of the computer code of this study compared with those of Jahanshahi et al. [8], both obtained using experimentally measured variable thermal conductivity. It should be noted that the values for average Nusselt numbers have been picked from a curve in [8] with ultimate care. As seen, for every volume fraction of nanoparticles good agreement exists between the average Nusselt number obtained in this study and that of Jahanshahi et al. [8].

Table 2

Nu_{avg} for $Ra=10^5$; comparison with [8] for validating the numerical results.

Φ	Nu_{avg} (Jahanshahi et al. [8])	Nu_{avg} (Present study)
0.01	4.83	4.82399
0.02	4.91	4.91729
0.03	5.05	5.02668
0.04	5.15	5.15333

5.2. Grid independency study

In order to use a proper grid in the numerical simulations, a grid independency study has been undertaken first. Seven different uniform grids of 41×41, 61×61, 81×81, 101×101, 121×121, 141×141 and 161×161 have been employed to simulate the natural convection of variable properties Al₂O₃-EG-w in the cavity for $\Phi=0.03$ and $Ra=10^5$. The variation of the average Nusselt number with the number of grids is presented in Table 3. As it can be observed, uniform grid of 141×141 is sufficiently fine to ensure

grid independent solutions. Hence, this grid has been used to perform all of the subsequent simulations.

6. Results and discussion

In this section, a representative set of graphical results are presented to illustrate the influence of different parameters on natural heat transfer characteristics of the mixture of 60:40 EG-w containing Al_2O_3 nanoparticles. The right wall has been maintained at the constant temperature of 298 K, whereas the temperature of the left wall has been changed dependent on Rayleigh number. In simulations for the variable properties cases, all of the thermophysical properties of nanofluid and base fluid have been considered variable. However, the Rayleigh number is based on the properties at the mean of the hot and cold temperatures.

In natural convection problems, when the density is considered variable with temperature, studying the term $\rho\psi$ which is called the flow strength is worthy not the streamlines. The flow strength depends on variation of both ρ and ψ ; thus better presents the effects of favoring and opposing forces. However, in [17-18] in which density has been considered constant the streamlines have been presented. In Fig. 2 the contour maps of ψ have been presented for Al_2O_3 -EG-water nanofluid and the base fluid for $\Phi = 0.001$ and 0.04 and $Ra = 10^3$, 10^5 and 10^7 . The flow is characterized by one rotating cell within the enclosure in all of the cases.

It is evident that increasing Rayleigh number results in higher intensity of the flow strength. This in turn strengthens the natural convection and improves the heat transfer rate. The presence of nanoparticles with $\Phi = 0.001$ has insignificant effect on the flow strength at $Ra = 10^3$ and 10^5 , but as Ra increases to 10^7 its effects become evident. However, the change of the maximum flow strength become more evident as Φ increases to 0.04 , such that at $Ra = 10^3$ the flow strength decreases but at $Ra = 10^5$ and 10^7 it adversely increases.

The nanofluid density increases with increase in volume fraction of nanoparticles but decreases with increase in temperature. On the other hand, due to viscosity increase, the stream function decreases with increased volume fraction of nanoparticles but it increases with temperature increase. At $Ra = 10^3$, for which convection is very weak, Ψ decreases sharply as Φ increases, however at $Ra = 10^5$ and 10^7 the

relative effect of density increase with Φ increase is greater than decrease of Ψ with Φ increase; thus the maximum flow strength increases. As was discussed here, ρ and Ψ show different responses to change of temperature and volume fraction of nanoparticles; this was not possible to be observed in [17-18].

Fig. 3 presents the y -velocity component for Al_2O_3 -EG-water nanofluid at mid-section of the square cavity ($y=0.5$) for $Ra = 10^3$ and 10^5 . Increasing the volume fraction of nanoparticles increases the effective viscosity of nanofluid and tends to slow down the movement of the fluid in the cavity; hence the magnitude of the vertical velocity decreases as Φ increases.

To illustrate how the thermal boundary layer thickness adjacent to the hot wall is influenced by the addition of nanoparticles, the isotherms for the base fluid as well as nanofluid with $\Phi = 0.001$ and 0.04 are presented in Fig. 4.

For $\Phi = 0.001$ there is not any noticeable change for the isotherms as well as thermal boundary layer close to the hot wall for nanofluid compared with the base fluid. However, as it increases to 0.04 the isotherms and the thermal boundary layer thickness show their sensitivity to the volume fraction of nanoparticles. This behavior is related to the increased viscosity as volume fraction of nanoparticles increases. The growth in thermal boundary layer thickness at $Ra = 10^5$ and 10^7 is responsible for the lesser temperature gradient at the hot wall which lowers the rate of the heat transfer accordingly. However, for $Ra = 10^3$ the volume fraction increase causes the thermal boundary layer thickness to increase at $y < 1/2$ and to decrease at $y > 1/2$, hence isotherms start to straighten up near the hot wall. In fact, at $\Phi = 0.04$ the isotherms become closer to the hot wall for $y > 1/2$, but they spread away from it and exhibit a trend almost similar to conduction in solids for $y < 1/2$. This behavior leads to the heat transfer enhancement for $y > 1/2$ and its decline for $y < 1/2$.

Fig. 5a-c show the variation of the local Nusselt number (Nu) along the hot wall for various values of nanoparticles volume fractions ($0 \leq \Phi \leq 0.04$) and $Ra = 10^3$, 10^5 and 10^7 . It is seen that for $Ra = 10^5$ and 10^7 increasing the volume fraction of nanoparticles leads to reduction of Nu . This behavior, which was discussed earlier, contradicts the results of some previous studies [5-8] for constant properties nanofluids, but agrees with variable properties results of Abu-Nada and Chamkha [17] for CuO-EG-water

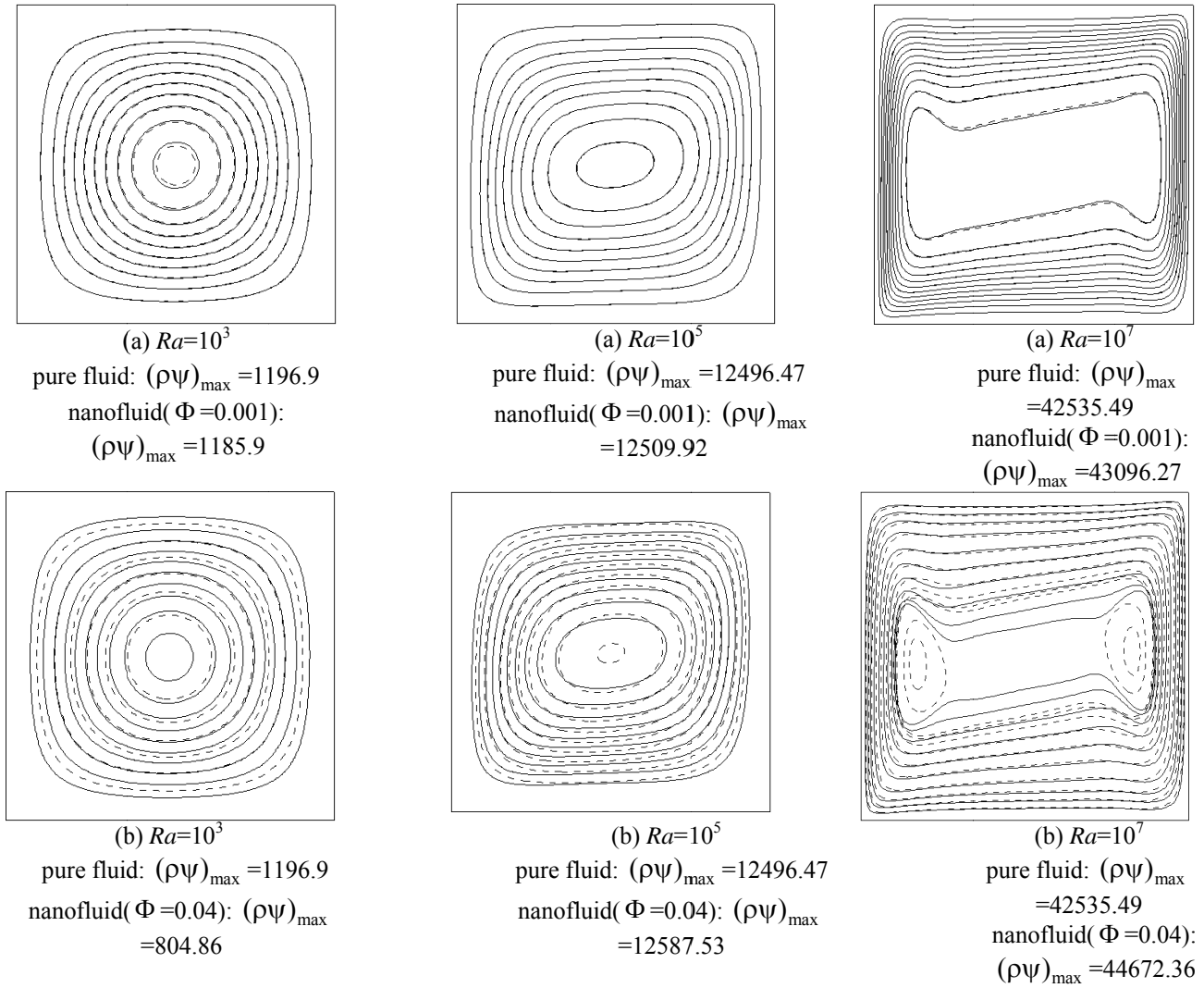


Fig. 2. Flow strength for the nanofluid for (a) $\Phi = 0.001$ and (b) $\Phi = 0.04$ (dashed lines) and the base fluid (solid lines).

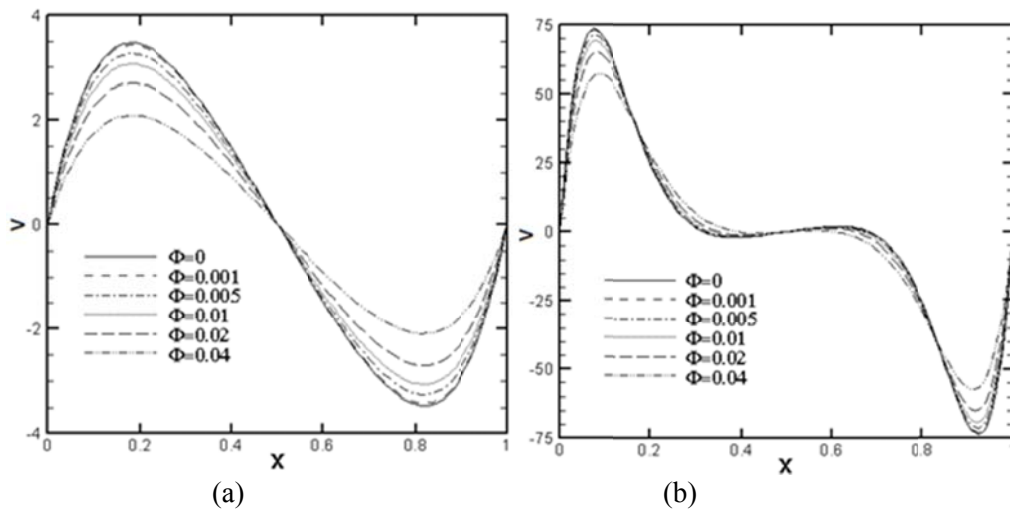


Fig. 3. y-velocity component at the midsection of the enclosure ($y=0.5$) for various Φ at: (a) $Ra=10^3$ (b) $Ra=10^5$

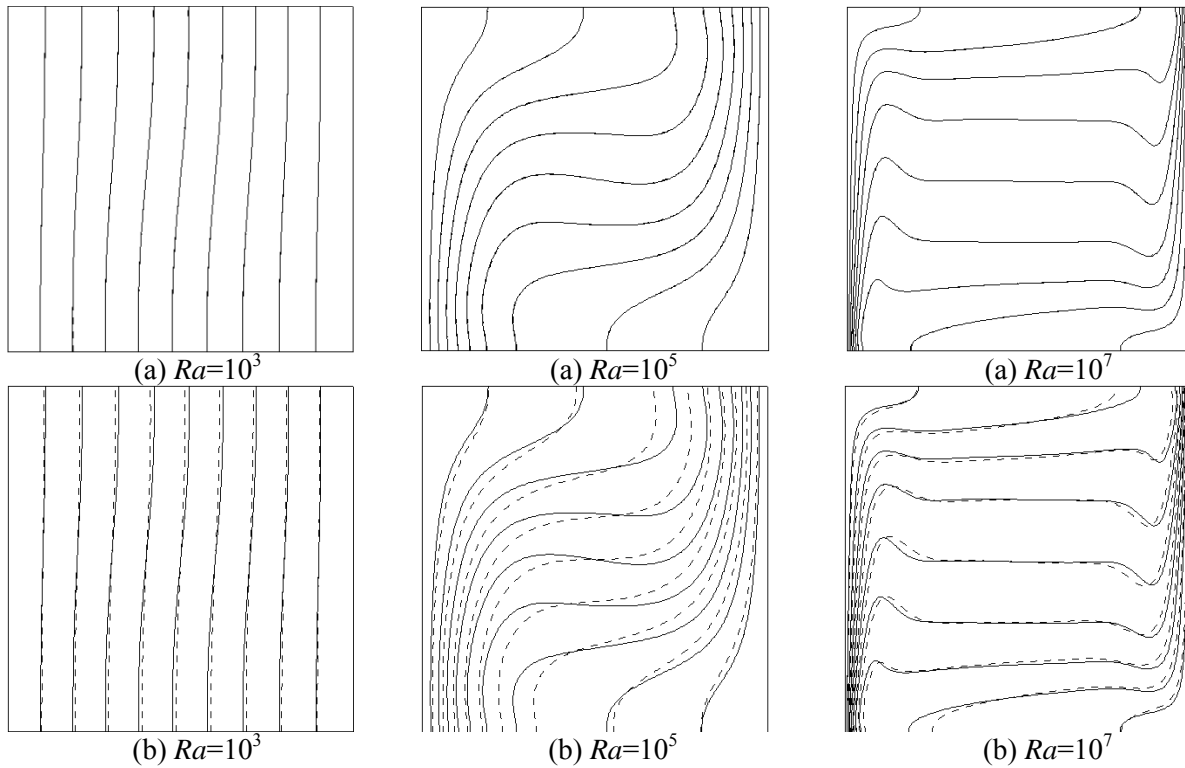


Fig. 4. Isotherms for the base fluid (solid lines) and the nanofluid (dashed lines) for (a) $\Phi=0.001$ (b) $\Phi=0.04$.

nanofluid and Abu-Nada et al. [18] for CuO-water nanofluid. However, for $Ra=10^3$ increasing the volume fraction of nanoparticles results in reduction of local Nusselt number at $y < 1/2$ but enhancement of Nu at $y > 1/2$.

Fig. 6a and 6b show the average Nusselt number and the Nusselt number ratio on the hot wall, respectively. For every volume fraction, Nu_{avg} increases with increasing Ra . For instance for $\Phi=0.04$ the values of Nu_{avg} at $Ra=10^5$ and 10^7 are 3.6 and 15.3 times greater than that of $Ra=10^3$, respectively. However, as Φ increases Nu_{avg} decreases for $Ra \geq 10^4$ but increases for $Ra=10^3$. Similarly at $Ra=10^3$, for which conduction heat transfer is dominant, the Nusselt number ratio on the hot wall has increased with increased Φ but for $Ra=10^4$ it has decreased with increased Φ . However, for $Ra=10^7$ compared to $Ra=10^4$, 10^5 and 10^6 the least deterioration in Nusselt number ratio has occurred as Φ has increased. As was presented in introduction, Abu-Nada et al [18] noticed different heat transfer behavior for Al_2O_3 -water nanofluid. This may be due to the fact that β , ρ and c_p were considered constant in their study.

Natural convection heat transfer is affected by change of Ra as well as nanofluid properties,

specifically nanofluid viscosity and thermal conductivity. In general, adding nanoparticles to the base fluid has two opposite effects on heat transfer: a positive effect due to presence of high thermal conductivity nanoparticles and an adverse effect promoted by increased effective viscosity of nanofluid. Enhancement of thermal conductivity of the nanofluid at $Ra=10^7$ compared to $Ra=10^3$, shown in Fig. 7, is related to increased Brownian motion. However, as Ra increases convection enhances and the relative effect of viscosity increase with Φ becomes less than that of conductivity enhancement; thus the relative decrease of Nu_{avg} decreases with increased Ra . This is why the least deterioration of Nu_{avg} occurs at $Ra=10^7$.

In [17-18] the reason for observed enhancement or deterioration of Nu_{avg} has not been explained, instead some general explanations have been presented. Nevertheless, this needs a quantitative analysis which is performed here. According to equation (15), the Nusselt number is influenced by temperature gradient at the left hot wall as well as thermal conductivity ratio. As shown in Fig. 8a, at $Ra=10^3$, for which conduction is dominant, as Φ increases the effect of increased thermal conductivity

becomes more important; thus Nu_{avg} increases. On the other hand, at $Ra=10^7$ as nanofluid viscosity increases with increased Φ the temperature gradient on the heated wall decreases, thus Nu_{avg} decreases. For the nanofluid with $\Phi=0.04$ compared to the base fluid there are 13.7 and 16.3% increase for thermal conductivity ratio and maximum 11.3 and 20.6% decrease for temperature gradient at $Ra=10^3$ and $Ra=10^7$, respectively (see Figs. 7 and 8).

In order to verify the observed trend of changing Nu_{avg} with Ra and Φ , in Fig. 9 the values of Nu_{avg} obtained in the present study have been compared with experimental results of [13, 31]. Although, the nanoparticles or the base fluid used in the mentioned experimental works differ from what has been used in the present study, the trend of changes is similar. This similarity is another verification of the results of this study.

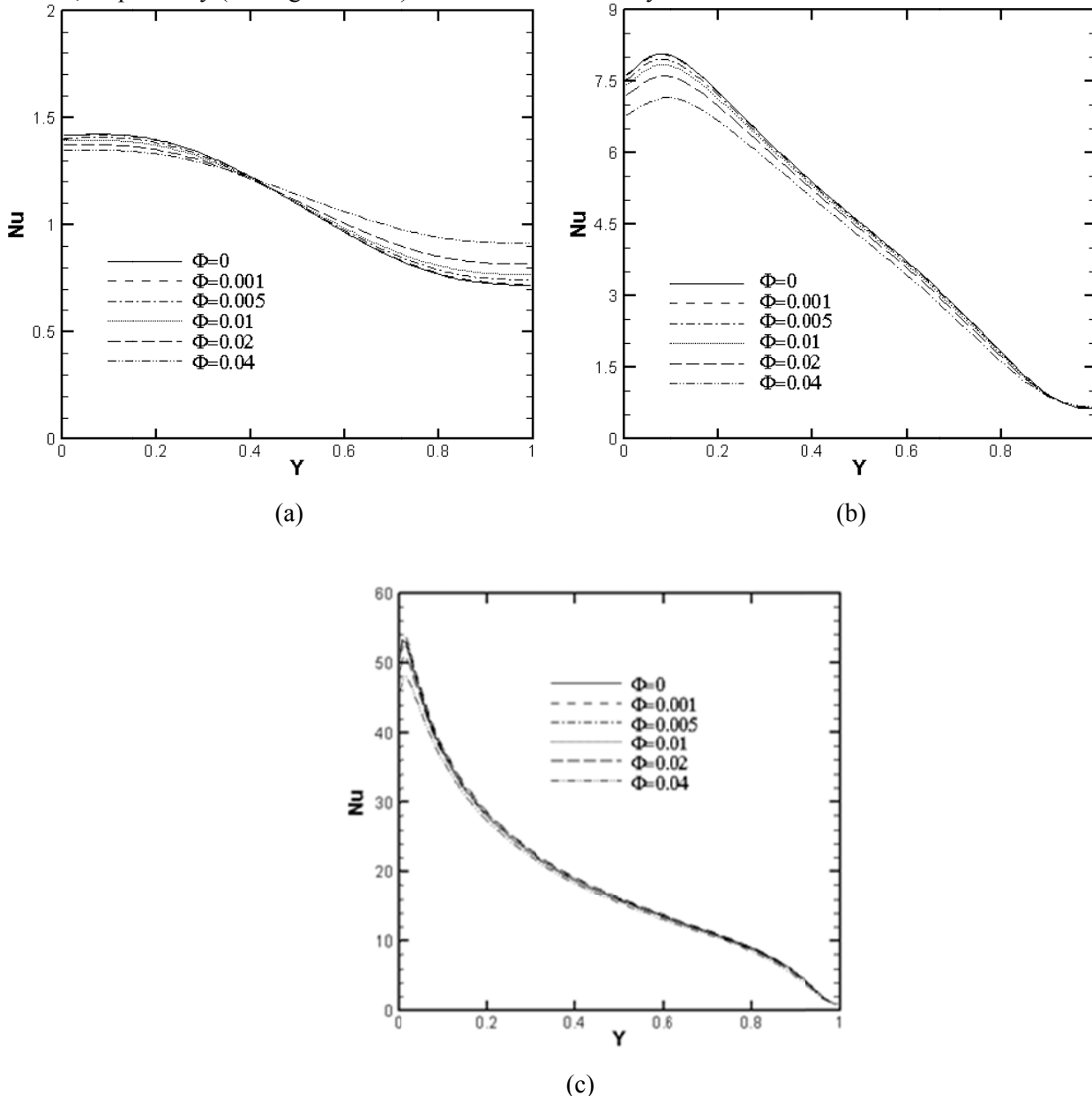


Fig. 5. Nu along the hot wall (a) $Ra=10^3$, (b) $Ra=10^5$, (c) $Ra=10^7$.

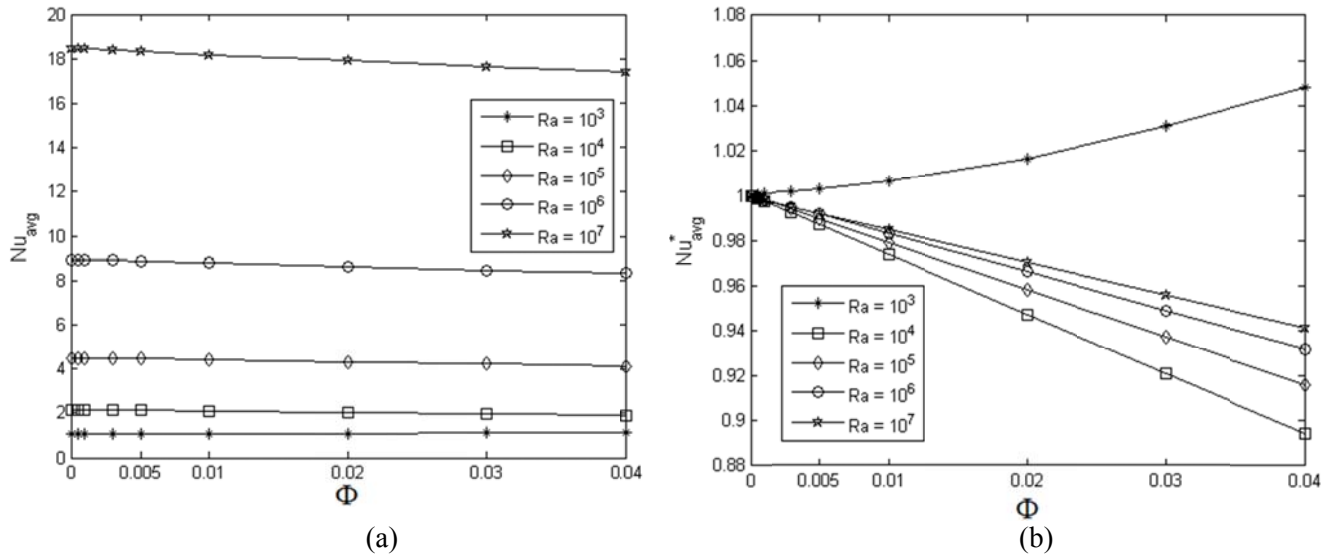


Fig. 6. (a) Average Nusselt number, (b) Nusselt number ratio.

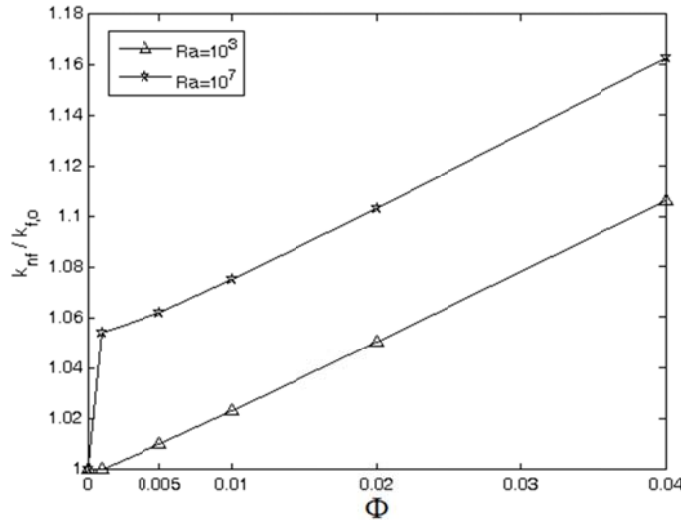


Fig. 7. Thermal conductivity ratio.

Fig. 10 shows Nu_{avg} for $Ra=10^7$ obtained in simulations for variable as well as constant properties models of this study. The properties in constant properties model (given by Eqs. 18-22) have been evaluated at the reference temperature of 300 K. According to Fig. 10, as Φ increases Nu_{avg} increases in the constant properties model, but decreases in the variable properties model. The results for constant properties model are in agreement with the results of previous numerical studies [5-8, 11], in which constant properties have been used. However, this trend contradicts the results of the present study for variable properties model and disagrees with experimental results reported by [12, 13, 31]. This experimental results reported by [12, 13, 31].

This distinction is due to underestimation of viscosity of the nanofluid in the constant properties models and states the important effects of temperature dependency of thermophysical properties.

In order to arrive at a clear conclusion about the disagreements on the effects of variation of properties on heat transfer a comparative study of the Al_2O_3 -EG-water nanofluid Rayleigh number with the base fluid Rayleigh number at various volume fractions and temperatures is presented here.

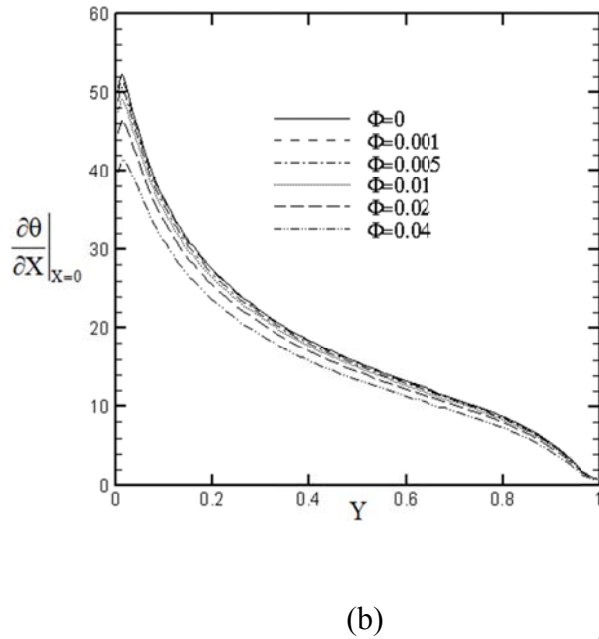
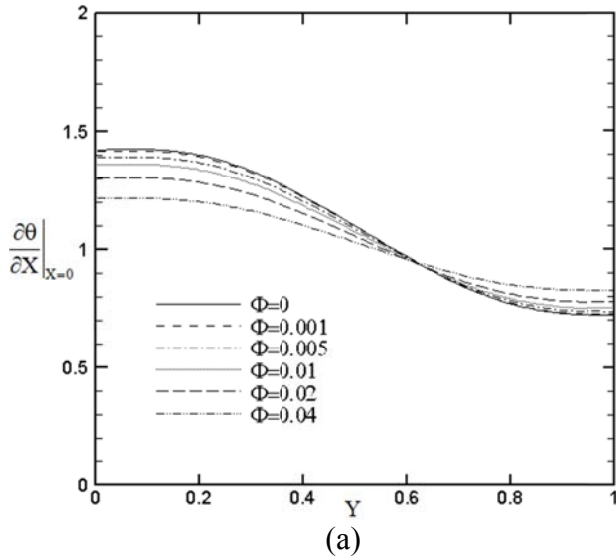


Fig. 8. Temperature gradient on the hot wall; (a) $Ra=10^3$
(b) $Ra=10$

Based on the scale analysis proposed by Bejan [32] the viscous force and the buoyancy force per unit mass, respectively, are:

$$\text{Viscous force} = \frac{\nu k}{L^3 \rho c_p} \quad (35)$$

$$\text{Buoyancy force} = g \beta \Delta T \quad (36)$$

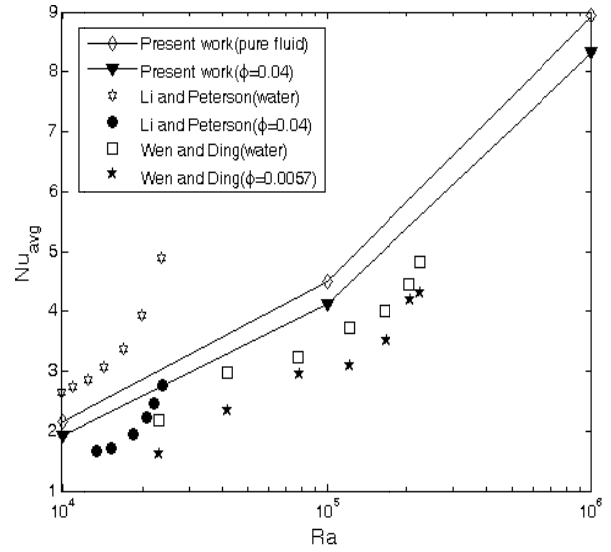


Fig. 9. Nu_{avg} in the experiments of Li and Paterson [13], Wen and Ding [31] and in the present numerical study.

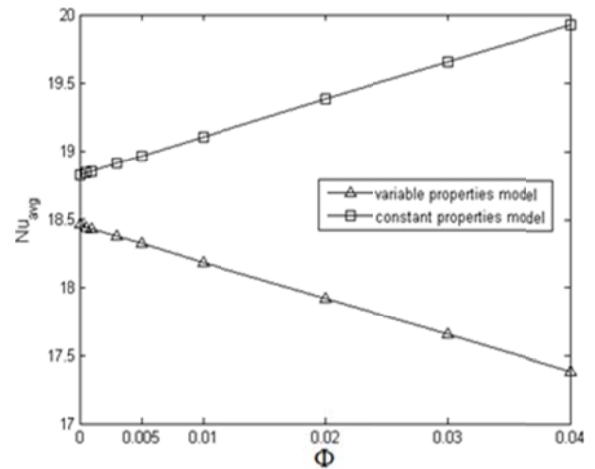


Fig. 10. Nu_{avg} for $Ra=10^7$; comparison between results of constant and variable properties models.

And the nanofluid Rayleigh number is:

$$Ra_{nf} = \frac{g \beta_{nf} L^3 (T_H - T_C)}{\alpha_{nf} \nu_{nf}} \quad (37)$$

Considering the same geometry and the same hot and cold temperatures, the Rayleigh number ratio becomes:

$$\frac{Ra_{nf}}{Ra_f} = \frac{\beta_{nf}\alpha_f\nu_f}{\beta_f\alpha_{nf}\nu_{nf}} \quad (38)$$

Eq. (38) is dependent only on the properties of the nanofluid and the base fluid at a nominated temperature. Therefore, it is representing the general state of natural convection in the cavity as both volume fraction of nanoparticles and temperature change. In order to study the effect of volume fraction of nanoparticles on the Rayleigh number ratio at a constant temperature, the properties in Eq. (38) were all evaluated at 300 K while Φ was changed step by step from 0.0 to 0.04. As shown in Fig. 11, the Rayleigh number ratio is smaller than one even for $\Phi = 0.001$ and as Φ increases it decreases further. This is due to the fact that the viscous force in the nanofluid enhances as the volume fraction of nanoparticles increases.

This phenomenon was reported in experimental studies of [12, 13, 31] and in the theoretical study of Hwang et al. [33] and is stating that for a case with constant cold and hot wall temperatures the strength of convection decreases as the volume fraction of nanoparticles increases. The variation of Rayleigh number ratio with average temperature is shown in Fig. 12 for two methods of evaluating the base fluid Rayleigh number.

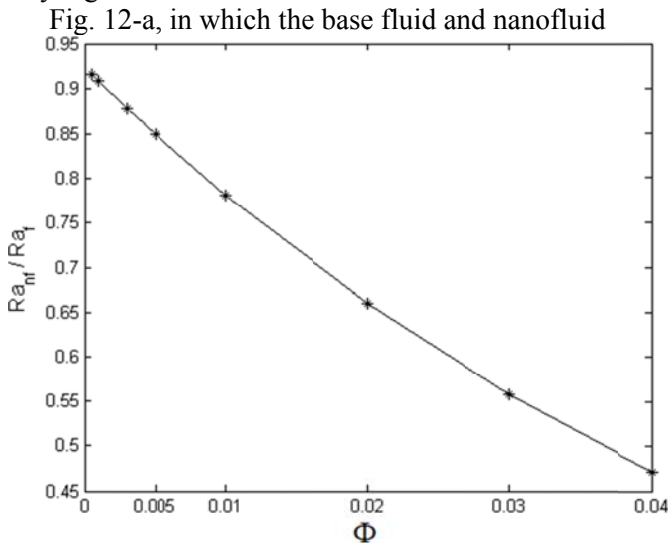


Fig. 11. Rayleigh number ratio (base fluid and nanofluid properties evaluated at 300 K).

Rayleigh numbers are based on properties at average hot and cold temperature, shows that Rayleigh number ratio is decreased gently as the average temperature is increased. Hwang et al. [33] for presenting their results used the same method for evaluating the base fluid Rayleigh number and concluded that the average Nusselt Number decreases with increasing Φ . However, in other numerical studies (e.g. Khanafer and Vafai [16]), in which heat transfer enhancement with increasing Φ has been reported, the base fluid Rayleigh number has been evaluated at a reference temperature. Fig. 12-b, in which the nanofluid Rayleigh number is based on the average temperature but the base fluid Rayleigh number is based on properties at reference temperature, shows that the Rayleigh number ratio increases as the average temperature of the nanofluid increases. An important observation from Fig. 12a-b is that as the volume fraction of nanoparticles increases the Rayleigh number ratio decreases. Fig. 12b shows that at $\Phi = 0.04$ the Rayleigh number ratio is smaller than one in the whole temperature range of 298-318 K. However for other volume fractions, the Rayleigh number ratio is smaller than one at lower mean temperatures and as the mean temperature increases it becomes greater than one. It should be noted that the effective thermal conductivity of a nanofluid is remarkably increased with temperature [20], which in turn increases the viscous force in the nanofluid (Eq. 35). It means the nanofluid Rayleigh number is less than that of base fluid at low mean temperatures but as mean temperature grows up it may become higher than that of base fluid. The average Nusselt number ratio is dependent on the Rayleigh number ratio. Therefore, it is concluded that different kinds of evaluation of the base fluid Rayleigh number in previous studies has led to observation of two opposite trends for nanofluid heat transfer behavior as volume fraction of nanoparticles increases.

7. Conclusions

The natural convection in an enclosure filled with an Al_2O_3 -EG-water nanofluid with variable properties was studied numerically. Various nanoparticles volume fractions and Rayleigh numbers have been considered and the flow and temperature fields as well as heat transfer characteristics have been studied.

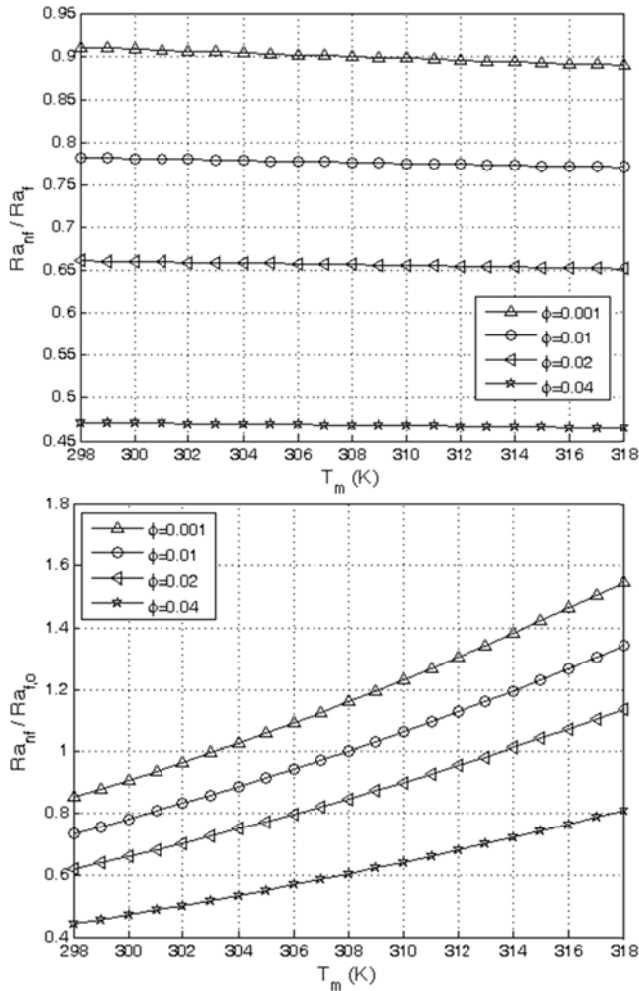


Fig. 12. Rayleigh number ratio; (a) Ra_f evaluated at $(T_H + T_C)/2$ (b) $Ra_{f,0}$ evaluated at T_0 .

The results showed for $Ra \geq 10^4$ and as the volume fraction of nanoparticles increases deterioration in heat transfer occurs compared to the base fluid heat transfer. This decrease is linked to increased viscosity as volume fraction of nanoparticles increases. However, by studying the Nusselt number it was noticed that this reduction is more severe at Ra of 10^4 compared to higher Ra of 10^5 , 10^6 or 10^7 such that the least deterioration in heat transfer occurs at $Ra=10^7$. At $Ra=10^3$ conduction heat transfer is dominant but as Ra increases further, convection enhances and due to increased Brownian motion, relatively more enhancement of thermal conductivity occurs. Thus, for higher Ra values the relative effect of the viscosity increase with Φ becomes less compared to the effect of conductivity enhancement. The heat transfer results of this study were verified by making comparison with experimental results of [13,33]. Also, the heat transfer results for variable properties

models were compared with the results obtained for constant properties models. Similar with the results of some previous numerical works [5-8,11], obtained using constant properties, the constant properties models of this study predicted heat transfer enhancement as Φ increased. It was shown that different kinds of evaluation of the base fluid Rayleigh number for variable properties nanofluid in previous studies has led to observation of heat transfer enhancement or deterioration with increasing volume fraction of nanoparticles.

Acknowledgements

The authors wish to thank the Energy Research Institute of the University of Kashan for supporting this research (Grant No. 158576/4).

References

- [1] X.Q. Wang, A.S. Mujumdar, Heat transfer characteristics of nanofluids: a review, *International Journal of Thermal Science* 46 (2007) 1-19.
- [2] J. Choi, Y. Zhang, Numerical simulation of laminar forced convection heat transfer of Al_2O_3 -water nanofluid in a pipe with return bend, *International Journal of Thermal Science* 55 (2012) 90-102.
- [3] P.K. Namburu, D.K. Das, K.M. Tanguturi, R.S. Vajjha, Numerical study of turbulent flow and heat transfer characteristics of nanofluids considering variable properties, *International Journal of Thermal Science* 48 (2009) 290-302.
- [4] R.J. Goldstein, W.E. Ibele, S.V. Patankar, T.W. Simon, T.H. Kuehn, P.J. Strykowski, K.K. Tamma, J.V.R. Heberlein, J.H. Davidson, J. Bischof, F.A. Kulacki, U. Kortshagen, S. Garrick, V. Srinivasan, K. Ghosh, R. Mittal, Heat transfer-A review of 2005 literature, *International Journal of Heat and Mass Transfer* 53 (2010) 4397-4447.
- [5] K. Khanafer, K. Vafai, M. Lightstone, Buoyancy-driven heat transfer enhancement in a two-dimensional enclosure utilizing nanofluids, *International Journal of Heat and Mass Transfer* 46 (2003) 3639-3653.
- [6] K.C. Lin, A. Violi, Natural convection heat transfer of nanofluids in a vertical cavity: Effects of non-uniform particle diameter and

- temperature on thermal conductivity, *International Journal of Heat and Fluid Flow* 31 (2010) 236-245.
- [7] G.A. Sheikhzadeh, A.Arefmanesh, M.H. Kheirkhah, R. Abdollahi, Natural convection of Cu–water nanofluid in a cavity with partially active side walls, *European Journal of Mechanics - B/Fluids* 30 (2011) 166-176.
- [8] M. Jahanshahi, S.F. Hosseinizadeh, M. Alipanah, A. Dehghani, G.R. Vakilnejad, Numerical simulation of free convection based on experimental measured conductivity in a square cavity using Water/SiO₂ nanofluid, *International Communications in Heat and Mass Transfer* 37 (2010) 687-694.
- [9] A.K. Santra, S. Sen, N. Chakraborty, Study of heat transfer characteristics of copper-water nanofluid in a differentially heated square cavity with different viscosity models, *Journal of Enhanced Heat Transfer* 15 (2008) 273-287.
- [10] C.J. Ho, M.W. Chen, Z.W. Li, Numerical simulation of natural convection of nanofluid in a square enclosure: Effects due to uncertainties of viscosity and thermal conductivity, *International Journal of Heat and Mass Transfer* 51 (2008) 4506-4516.
- [11] E. Abu-Nada, Z. Masoud, A. Hijazi, Natural convection heat transfer enhancement in horizontal concentric annuli using nanofluids, *International Communications in Heat and Mass Transfer* 35 (2008) 657-665.
- [12] N. Putra, W. Roetzel, S.K. Das, Natural convection of nano-fluids, *Heat and Mass Transfer* 39 (2003) 775-784.
- [13] C.H. Li, G.P. Peterson, Experimental studies of natural convection heat transfer of Al₂O₃/DI water nanoparticle suspensions (Nanofluids), *Advances in Mechanical Engineering* (2010) doi:10.1155/2010/742739.
- [14] C.J. Ho, W.K. Liu, Y.S. Chang, C.C. Lin, Natural convection heat transfer of alumina-water nanofluid in vertical square enclosures: An experimental study, *International Journal of Thermal Science* 49 (2010) 1345-1353.
- [15] A.G.A. Nnanna, Experimental model of temperature-driven nanofluid, *Journal of Heat Transfer* 129 (2007) 697-704.
- [16] K. Khanafer, K. Vafai, A critical synthesis of thermophysical characteristics of nanofluids, *International Journal of Heat and Mass Transfer* 54 (2011) 4410-4428.
- [17] E. Abu-Nada, A.J. Chamkha, Effect of nanofluid variable properties on natural convection in enclosures filled with a CuO-EG-Water nanofluid, *International Journal of Thermal Science* 49 (2010) 2339-2352.
- [18] E. Abu-Nada, Z. Masoud, H.F. Oztop, A. Campo, Effect of nanofluid variable properties on natural convection in enclosures, *International Journal of Thermal Science* 49 (2010) 479-491.
- [19] B.C. Sahoo, R.S. Vajjha, R. Ganguli, G.A. Chukwu, D.K. Das, Determination of rheological behavior of aluminum oxide nanofluid and development of new viscosity correlations, *Petroleum Science and Technology* 27 (2009) 1757-1770.
- [20] R.S. Vajjha, D.K. Das, Experimental determination of thermal conductivity of three nanofluids and development of new correlations, *International Journal of Heat and Mass Transfer* 52 (2009) 4675-4682.
- [21] R.S. Vajjha, D.K. Das, Specific heat measurement of three nanofluids and development of new correlations, *Journal of Heat Transfer* 131 (2009) 1-7.
- [22] R.S. Vajjha, D.K. Das, B.M. Mahagaonkar, Density measurement of different nanofluids and their comparison with theory, *Petroleum Science and Technology* 27 (2009) 612-624.
- [23] B.C. Pak, Y.I. Cho, Hydrodynamic and heat transfer study of dispersed fluids with submicron metallic oxide particles, *Experimental Heat Transfer* 11 (1999) 151-170.
- [24] Y. Xuan, W. Roetzel, Conceptions for heat transfer correlation of nanofluids, *International Journal of Heat and Mass Transfer* 43 (2000) 3701-3707.
- [25] H.C. Brinkman, The viscosity of concentrated suspensions and solutions, *Journal of Chemical Physics* 20 (1952) 571.
- [26] X. Wang, X. Xu, S.U.S. Choi, Thermal conductivity of nanoparticle–fluid mixture, *Journal of Thermophysics and Heat Transfer* 13 (1999) 474–480.
- [27] ASHRAE Handbook, Fundamentals. American Society of Heating, Refrigerating and Air-Conditioning Engineers Inc., Atlanta, GA, 2005.

- [28] F.P. Incropera, D.P. DeWitt, Introduction to Heat Transfer, third ed. John Wiley & Sons, Inc., New York, 1996.
- [29] R.S. Vajjha, D.K. Das, D.P. Kulkarni, Development of new correlations for convective heat transfer and friction factor in turbulent regime for nanofluids, International Journal of Heat and Mass Transfer 53 (2010) 4607-4618.
- [30] S.V. Patankar, Numerical Heat Transfer and Fluid Flow, McGraw-Hill, 1980.
- [31] D. Wen, Y. Ding, Natural Convective Heat Transfer of Suspensions of Titanium Dioxide Nanoparticles (Nanofluids), IEEE Transactions on Nanotechnology 5 (2006) 220-227.
- [32] A. Bejan, Convective Heat Transfer, second ed. John Wiley & Sons, New York, 1995.
- [33] K.S. Hwang, J.H. Lee, S.P. Jang, Buoyancy-driven heat transfer of water-based Al₂O₃ nanofluids in a rectangular cavity, International Journal of Heat and Mass Transfer 50 (2007) 4003-4010.